5th INTERNATIONAL CONFERENCE ON MECHATRONICS TECHNOLOGY (ICMT2001)
June 6-8, 2001, National University of Singapore

KINEMATIC PERFORMANCE COMPARISON OF LINEAR TYPE PARALLEL MECHANISMS APPLICATION TO THE DESIGN AND CONTROL OF A HEXASLIDE

Patrick HUYNH
Email: huynh@np.edu.sg

NgeeAnn Polytechnic
Mechanical Engineering Department
535 Clementi Road, 599489 Singapore

ABSTRACT

Kinematic performance characteristics for parallel mechanisms in terms of working space volume, singularity points and maximum velocity are presented. Using these performance characteristics which are basically important issues in kinematic design and control of parallel manipulators, the performance comparison can be made between a 6 d.o.f conventional Gough-Stewart Platform (GSP) and a 6 d.o.f Hexaslide Parallel Mechanism (HPM) with fixed linear actuators. This study can serve as a basic guide for the design of parallel manipulators in the sense of achieving kinematic performances, and has been applied to the design and motion control of the Hexaslide.

KEY WORDS: *Parallel Mechanism, Workspace, Singularity, Maximum Velocity, Kinematic Performance, Motion Control.*

1 INTRODUCTION

In order to design a high performance motion controlled parallel manipulators, kinematic performance characteristics of parallel mechanisms in terms of workspace volume, singular configurations and maximum velocity are investigated. There are many other performance characteristics based on kinematics [1]. Here, workspace, singularities and velocity zones are only considered because they are basically important issues in kinematic design and control of parallel manipulators.

In this paper, the methods allowing to determine these characteristics are briefly presented. They have been developed and particularly applied to parallel manipulators. The working space of a manipulator is one of the most important specifications for the designers, as it can be used to evaluate the kinematic performance of a designed robotic mechanism [2-6]. For example, J.P. Merlet [4] compares four different parallel robot geometries based on their numerical workspace volumes and shows that for robot of similar dimensions the joints layout has a large influence on the workspace volume. Clément M. Gosselin et al. [5] use one of their comparison criteria which is the working volume in Cartesian space to compare four different architectures of 6 d.o.f parallel mechanisms. Their results show that although different architectures have certain advantages in specific performance measures, the Gough-Stewart platform offers the most balanced performance. F.C. Park et al. [6] analyse the machine tool workspace by introducing a volume form on the space of homogeneous transformations, in order to compare for CNC machining applications the kinematic performance of the 6 d.o.f conventional Gough-Stewart platform and a hybrid 6 d.o.f serial-parallel structure called 3-PRPS. In general, the positioning workspace volume of the 3-PRPS Mechanism is much larger than that of the Gough-Stewart platform assuming machines of approximately the same physical dimension. Different methods to determine the workspace of a parallel mechanism have been proposed by many researchers, either by using a numerical method [7,8,9], or a geometrical algorithm [10,11]. Here, we use the numerical procedure based on a complete discretization of the Cartesian space to calculate the workspace volume for a fixed orientation and altitude of the mobile platform. Singular configurations are identified by using Grassmann geometry approach which has been proposed by Merlet [12,13] in order to find all the singular configurations of a parallel mechanism. Finally, the determination of the maximum velocity is based on the analysis of the algebraic inequalities describing the constraints on the kinematics model [14].

Using these performance characteristics, the comparison and evaluation can be made between a 6 d.o.f conventional Gough-Stewart Platform (GSP) which has been well known as a moving linear type parallel mechanism [15], and a 6 d.o.f Hexaslide Parallel Mechanism (HPM) which is considered as a new type parallel mechanism with fixed linear actuators [16]. By taking merits of simulation results, a Hexaslide prototype was designed and constructed in Japan and Korea for underground excavation and tire carving, and an optimal velocity based control method [17] for high speed straight line trajectory of the Hexaslide has been proposed. The proposed control algorithm is then implemented in real time trajectory planning and position servoing in order to satisfy the requirements in the actual manufacturing automation.

2 DETERMINATION OF THE WORKSPACE AREA AND VOLUME

We consider a general 6 d.o.f parallel mechanism represented in Fig.1. It is composed of 2 rigid bodies connected by 6 actuated variable-length links. The stationary body is referred to as the base (frame b) and the moving body is referred to as the mobile platform (frame m). The position and orientation of the mobile platform can be controlled with respect to the base by changing the 6 link lengths.

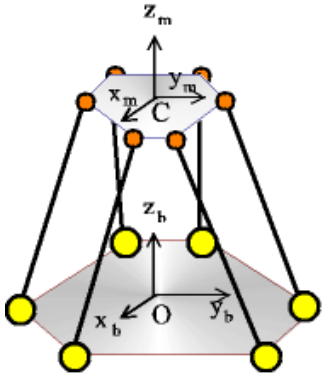

Fig.1: *A general 6 d.o.f parallel mechanism*

The factors, which limit the workspace of a parallel mechanism, are the limit of the link lengths, mechanical limits on the passive joints and the links interference. The algorithm to compute the workspace area and volume is described as follows.

- The orientation is fixed to normal direction (Z axis), i.e. three Euler angles are zeros.

- For a given Z height from Z_{min} to Z_{max} in ΔZ increments, the X-Y range of the area workspace A_z is computed. The area A_z is composed of N_θ "slices" from $\theta = 0$ to 2π in $\Delta\theta = 2\pi / N_\theta$ increments, and the radius r_z of each "slice" is incremented until the boundary is attained by solving the inverse geometry to determine the link lengths. After the link lengths are computed, they are first checked to verify the limit of the actuators motion range. Then, the configuration area is evaluated by taking into account the links interference and motion range of passive joints.

Thus,
$$A_z = \sum_{\theta=0}^{2\pi-\Delta\theta} \frac{\pi\, r_z^2(\theta)}{N_\theta}. \qquad (1)$$

- The total volume V is calculated as the sum of the incremental volumes of $A_z \,.\, \Delta Z$

Thus,
$$V = \sum_{Z=Z_{\min}}^{Z_{\max}} A_z \,.\, \Delta Z \,. \qquad (2)$$

3 DETERMINATION OF THE SINGULAR CONFIGURATIONS

A single Jacobian matrix $\boldsymbol{J}$ of general parallel mechanisms can be defined as

$$\dot{\vec{l}} = \boldsymbol{J}\, \dot{\vec{x}}, \qquad (3)$$

where $\dot{\vec{x}}$ is the end effector velocity vector and $\dot{\vec{l}}$ is the articular velocity vector. Singular configurations are determined by finding the roots of the symbolic determinant of $\boldsymbol{J}$ which is a huge non-linear expression, since each Jacobian element is quite complicated. Merlet [12,13] proposed an original method based on Grassmann line geometry which is briefly described in the followings.

A line Δ can be described by its 6 Plücker coordinates as $\vec{P}_\Delta = [S_x \;\; S_y \;\; S_z \;\; M_x \;\; M_y \;\; M_z]^T$, where $\vec{P}_\Delta$ is Plücker vector of the line Δ, $\vec{S} = [S_x \;\; S_y \;\; S_z]^T = \overrightarrow{M_1 M_2}$, $\vec{M} = [M_x \;\; M_y \;\; M_z]^T = \overrightarrow{OM_1} \wedge \overrightarrow{OM_2} = \overrightarrow{OM_1} \wedge \vec{S} = \overrightarrow{OM_2} \wedge \vec{S}$. $\wedge$ is the cross product of two vectors, M_1 and M_2 are two points belonging to Δ in the reference frame $\Re_o$ whose origin is o (Fig. 2).

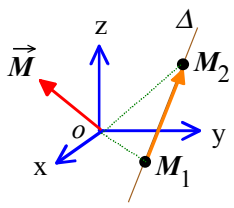

Fig.2: *Plücker coordinates representation*

The normalized vector is defined as

$$\vec{P}'_\Delta = \frac{\vec{P}_\Delta}{\|\vec{S}\|} = [S'_x \;\; S'_y \;\; S'_z \;\; M'_x \;\; M'_y \;\; M'_y]^T.$$

Let $\vec{F}$ be the force vector in operational space acting on the mobile platform and $\vec{f} = [f_1 \cdots f_6]^T$ articular force vector in the links. It has been shown in [12] that $\vec{F} = \boldsymbol{J}^T \vec{f}$ and the Jacobian matrix $\boldsymbol{J}$ is defined as $\boldsymbol{J} = [\vec{P}'_1 \cdots \vec{P}'_6]^T$, where $\vec{P}'_i$ is the normalized Plücker coordinates vector of line i (i = 1,6) associated to the link i and defined as

$$\vec{P}'_i = \begin{bmatrix} \vec{z}_i \\ \overrightarrow{CB_i} \wedge \vec{z}_i \end{bmatrix}, \qquad (4)$$

where
- $\vec{z}_i$: unit vector of the link i,
- C : origin point of the mobile platform frame,
- B_i : attachment point i of the mobile platform,
- $\wedge$: cross product of two vectors.

Consequently, a singular configuration of a parallel mechanism corresponds to a configuration where the rank of the matrix Jacobian $\boldsymbol{J}$ is less than 6, i.e. the 6 Plücker vectors $\vec{P}'_i$ (i = 1,6) can be described by the Grassmann geometry which consists of finding the geometric characterization of linear varieties of lines associated to the links of the parallel mechanism. Table 1 summarizes the geometrical description of Grassmann varieties of lines classified by rank from 1 to 5.

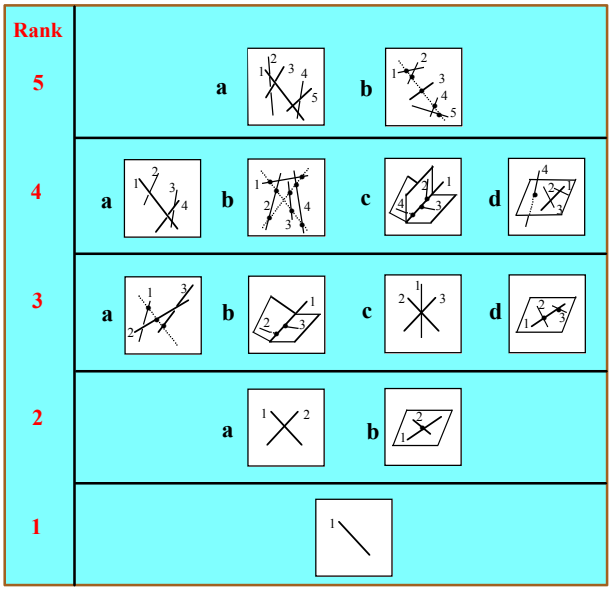

Table 1: *Linear varieties of line systems*

4 DETERMINATION OF THE MAXIMUM VELOCITY

We choose the bounded limit ρ of articular velocities $\dot{l}_i$ (i= 1,6), define the Jacobian $\boldsymbol{J}$ and the velocity $\dot{\vec{x}}$ of the mobile platform as follows: $\dot{l}_i \le \rho \;\; \forall i \in [1,6]$, $\boldsymbol{J} = (\!(c_{ij})\!)_{\substack{i=1,6 \\ j=1,6}}$ and $\dot{\vec{x}} = [v_x \;\; v_y \;\; v_z \;\; \omega_x \;\; \omega_y \;\; \omega_z]^T$, where c_{ij} is the i^{th} and j^{th} element of the Jacobian matrix $\boldsymbol{J}$, (v_x, v_y, v_z) are the three translational components and (ω_x, ω_y,

ω_z) three rotational components of the operational velocity. At every configuration point $\vec{x}_c = [x_c \quad y_c \quad z_c \quad \psi \quad \theta \quad \varphi]^T$ of the mobile platform where (x_c, y_c, z_c) are the three translational components of the position vector of the mobile platform and (ψ, θ, φ) three Euler angles defining the orientation of the mobile platform with respect to the fixed base, we try to find in the hyper-plane the frontier limiting possible velocities of the mobile platform. From Eq. **(3)**, every point of the permitted zone must satisfy the following constraints

$$-\rho \le c_{i1}.v_x + c_{i2}.v_y + c_{i3}.v_z + c_{i4}.\omega_x + c_{i5}.\omega_y + c_{i6}.\omega_z \le \rho \ . \qquad \textbf{(5)}$$

$\forall i \in [1,6]$, there are totally 12 constraint equations. Each equation defines a permitted half hyper-plane and the final zone is the intersection of these half hyper-planes.

It is difficult to imagine in six dimensions the nature of this intersection zone. Thus, in case of 2D we fix for example four components of the velocity and represent in a plane the frontier limiting two remaining components of velocity of the mobile platform. As an example, supposing $v_z = 0$ and $\omega_x = \omega_y = \omega_z = 0$, equation **(5)** yields

$$-\rho \le c_{i1}.v_x + c_{i2}.v_y \le \rho \qquad \forall i \in [1,6] \ . \qquad \textbf{(6)}$$

The solution $V_{max} = \left\| \vec{x}_{\max} \right\|$ corresponds to the summit of the polygon farthest from the origin of the velocity frame, and the norm of the vector from the origin to this summit represents V_{max}. From this method of construction, we can also build the volume of permitted velocity by drawing successive cuts for different values of a third component of operational velocity. This type of intersection in 3D may result in either an empty set, or a point, or a segment, or finally a polygon or a convex polyhedron.

Figure 3 shows in the (v_x, v_y) plane, lines defining the constraint equations **(6)** and the permitted polygonal zone.

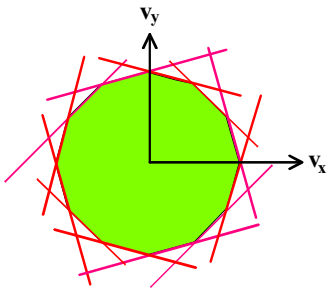

Fig. 3: *Permitted zone of operational velocity in* the (v_x, v_y) *plane*

5 APPLICATION TO PERFORMANCE COMPARISON AND CONTROL OF PARALLEL MECHANISMS

The mechanisms used in this example are the conventional Gough-Stewart Platform (GSP) and the Hexaslide Parallel Mechanism (HPM) with fixed linear actuators. For performance comparison study, the principal geometric parameters and the actuators of these two parallel mechanisms are assumed to be in the same range. They differ only from their mechanism architectures. The actuators used in GSP are mounted at the base of moving linkages, which have variable lengths, while those of the HPM are always fixed at the base and its moving linkages have the fixed lengths. The design parameters specifications of the HPM have been given in [16].

5.1 GOUGH-STEWART PLATFORM (GSP)

The geometric model of the GSP and its parameters are shown in Fig. 5. The inverse geometric model is derived by solving l_i representing the variable length of the link, for the given $\vec{p}$ (center location vector of the mobile platform) and $\mathfrak{R}$ (3 by 3 orthogonal matrix representing the orientation of the mobile platform with respect to the base) as follows.

$$l_i \vec{z}_i = \vec{p} + \vec{s}_i - \overrightarrow{OA_i} \ , \qquad \textbf{(7)}$$

where $\vec{z}_i$ is a unit vector of the link i ($i \in [1,6]$), $\vec{s}_i = \mathfrak{R}\left(\overrightarrow{CB_i}\right)_m$, $\left(\overrightarrow{CB_i}\right)_m$ is the position of the center of the spherical joint connecting link i to the mobile platform and expressed in the mobile platform frame m, and $\overrightarrow{OA_i}$ represents the position of the center of the universal joint connecting link i to the base platform. Fig. 6 shows a 3D view of the GSP manipulator workspace and its numerical volume from the simulation results.

Singular configurations can be found by using directly the results from Merlet [12] with the case of the Simplified Symmetric Manipulator (SSM). However, based on the GSP kinematic architecture, only a linear variety of type 5a has been found. In this case, the three lines belonging respectively to the three flat pencils spanned by the links (1,2), (3,4) and (5,6) and lying in the mobile platform plane intersect at a unique point M. Fig. 4 illustrates an example of this case.

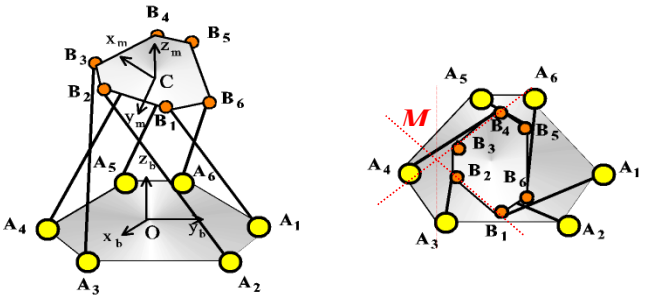

Fig. 4: *GSP singular configuration of type 5a*

$$\vec{x}_c = \left[0 \quad 0 \quad 0.569m \quad \frac{\pi}{2} \quad 0 \quad 0\right]^T$$

Analytically, we have

$$\begin{aligned} \left(\overrightarrow{A_1B_1} \wedge \overrightarrow{A_2B_2}\right) \cdot \overrightarrow{A_1M} = 0, \\ \left(\overrightarrow{A_3B_3} \wedge \overrightarrow{A_4B_4}\right) \cdot \overrightarrow{A_3M} = 0, \\ \left(\overrightarrow{A_5B_5} \wedge \overrightarrow{A_6B_6}\right) \cdot \overrightarrow{A_5M} = 0, \end{aligned} \qquad \textbf{(8)}$$

$$\overrightarrow{B_1M} \cdot \vec{n}_z = 0 \ . \qquad \textbf{(9)}$$

where $\vec{n}_z$ is the normal vector of the mobile platform. From relations **(8)** and **(9)**, a singular configuration occurs when $\psi = \pm\frac{\pi}{2}$, i.e. the mobile platform is rotated by $\pm\frac{\pi}{2}$ about the vertical axis and $\theta = \varphi = 0$ whatever is the position of the center of the mobile platform. This is the Fichter's intuitive singular configuration [18], which was also applied to the parallel link manipulator [7] and the modified Stewart

Platform [19]. Practically, the Jacobian matrix at the configuration $\vec{x}_c = \left[0 \quad 0 \quad 0.569m \quad \frac{\pi}{2} \quad 0 \quad 0\right]^T$ is

-0.7041	0.4074	0.5816	0.1404	0.0376	0.1437
-0.2840	0.6474	0.7073	0.0458	-0.1708	0.1747
0.7049	0.4061	0.5816	-0.0376	-0.1404	0.1437
0.7027	-0.0777	0.7073	-0.1708	0.0458	0.1747
-0.0008	-0.8135	0.5816	-0.1028	0.1028	0.1437
-0.4186	-0.5697	0.7073	0.1250	0.1250	0.1747

and its determinant is 7.5002e-19, very close to zero. At this configuration the third and the last columns of the Jacobian are proportional, so the Jacobian is not full rank and cannot be inverted. The detailed calculation of the Jacobian matrix $\boldsymbol{J}$ is given in [14].

Figure 7 presents from simulation results in 2D (v_x, v_y) view the velocity zones and the norm of the maximum operational velocity of the GSP in nominal position $\vec{x}_c = [0 \quad 0 \quad 0.569m \quad 0 \quad 0 \quad 0]^T$ with $\omega_x = \omega_y = \omega_z = 0$.

5.2 HEXASLIDE PARALLEL MECHANISM (HPM)

The geometric model of the HPM and its parameters are shown in Fig. 5. The inverse geometric model is derived by solving l_i, representing the variable length of the rail, when the position $\vec{p}$ and the orientation $\mathfrak{R}$ of the mobile platform are given as follows.

$$l_i \, \vec{a}_i + c \, \vec{z}_i = \vec{p} + \vec{s}_i - \overrightarrow{OA_i}, \qquad \textbf{(10)}$$

where $\vec{a}_i$ and $\vec{z}_i$ are unit vectors of the linkage i (i = 1,6), c is a fixed length of the moving linkage, and $\overrightarrow{OA_i}$ is the position of the center of the linear actuator i fixed on the base platform. The definition of other parameters is the same as in the GSP. Figure 6 shows a 3D view of the HPM workspace and its numerical volume from the simulation result. Based on the HPM kinematic architecture, all types of linear varieties in table 1 are not successively verified. The detailed calculation of $\boldsymbol{J}$ is given in [14].

Numerically, the determinant of the Jacobian matrix at the configuration $\vec{x}_c = \left[0 \quad 0 \quad 0.569m \quad \frac{\pi}{2} \quad 0 \quad 0\right]^T$ is -0.0039 (not zero). Thus, Fichter's singular configuration is not applicable to this parallel mechanism.

The 2D (v_x, v_y) view of the velocity zones and the norm of the maximum velocity of the HPM in nominal position $\vec{x}_c = [0 \quad 0 \quad 0.569m \quad 0 \quad 0 \quad 0]^T$, with $\omega_x = \omega_y = \omega_z = 0$, are presented in Fig. 7.

5.3 PERFORMANCE COMPARISONS AND CONTROL ISSUE

The nominal position of the two parallel manipulators is bounded by the largest workspace. The workspace of the HPM is larger than that of the GSP. Numerically, the volume of the HPM is almost twice than that of the GSP. This suggests that the HPM design offers much better dexterous working space than that of the GSP. Fichter's singularity is identified for the GSP but not for the HPM. In this case, the HPM is easily controllable over the GSP. Fig. 7 shows that the norms of maximum operational velocity of the two parallel mechanisms are very close. But the polygon of the HPM is close to a circle, while those of the GSP is exactly a hexagon. This suggests that the HPM has the most uniform and isotropic velocity zone, which can facilitate the fine position control from this nominal position.

Based on the good kinematic performance of HPM, the design and fabrication of the HPM has been launched and tested at Mechanical Engineering Laboratory, Japan. Through parallel mechanism design and direct drive actuators utilization, an optimal velocity control based on the maximum velocity analysis in operational space has been implemented in order to achieve a high speed straight line trajectory without considering degree of accuracy [17]. The hardware system and the control block diagram are illustrated in Fig. 9.

6 CONCLUSION

Kinematic performance characteristics of parallel mechanisms in terms of workspace volume, singular configurations and maximum velocity have been presented in this paper. Numerical procedure for the workspace area and volume calculation is given. The determination of the workspace is very useful for the designers to evaluate the kinematic properties and performances at the preliminary design stage. For example, Arai et al. [16] fixed the inclination angle of the rail in their new prototype to realize the largest workspace. Singular configurations are identified by utilizing the Grassmann geometry approach. The identification of the singularities represents an important issue in kinematic design and control of robotic mechanisms. Cleary and Arai [19] considered the Fichter's configuration of their prototype called Modified Steward Platform as outside of the manipulator's workspace and therefore the singularity does not interfere with the twisting operation about the z-axis. However, the workspace of their prototype must be reduced. The graphical method for computing the maximum velocity and its permitted zones of parallel mechanisms in operational space has been briefly presented. The advantage of this method is that the constraint equations are simple by just knowing the Jacobian matrix of the manipulator at a given configuration point. The drawing results allow the designer to achieve the kinematic optimal performance during trajectory generation and position control.

Based on these performance characteristics, a fictive conventional Gough-Stewart Platform (GSP) and a Hexaslide Parallel Mechanism (HPM) with fixed linear actuators can be evaluated for kinematic performance comparisons according to their workspace volume, singular configurations and maximum velocity zones. It has been shown that the HPM has got much better performance characteristics than those of the GSP. This study, it is believed, can serve as a basic guide for the design of parallel manipulators in the sense of achieving kinematic performances, and has been applied to the design and motion control of the Hexaslide Parallel Mechanism (HPM).

REFERENCES

[1] M. Uchiyama et al., "Performance Evaluation of Manipulators Using the Jacobian and Its Application to Trajectory Planning", *Robotics Research, The 2nd International Symposium*, MIT Press, 1985, pp.447-454.

[2] T.W. Lee and D.C.H. Wang, "On the Evaluation of Manipulator Workspace", *Transactions of the ASME, Journal of Mechanisms, Transmission, and Automation in Design*, Vol.105, March 1983, pp.70-77.

[3] J.P. Merlet, "Workspace-oriented methodology for designing a parallel manipulator", *Proceedings of the International Conference on Robotics and Automation*, Minneapolis, Minnesota, USA, April 1996, pp.3726-3731.

[4] J.P. Merlet, "Determination of 6D Workspace of Gough-Type Parallel Manipulator and comparison between different Geometries", *The International Journal of Robotics Research*, vol. 18, no. 9, pp. 902-916, Sept. 1999.

[5] C.M. Gosselin et al., "A Comparison of architectures of Parallel Mechanisms for Workspace and Kinematic Properties", *Proceedings of the ASME Design Automation Conference*, Boston, vol. DE-82, pp. 951-958, Sept. 1995.

[6] F.C. Park, et al., "Performance Analysis of Parallel Mechanisms Architectures for CNC Machining Applications", *International Mechanical Engineering Congress & Exposition*, MED vol. 6-2, ASME, Dallas, Nov. 16-21, 1997.

[7] T. Arai et al., "Development of a parallel link manipulator", *International Conference on Advanced Robotics (ICAR'91)*, Pise, Italy, June 1991, pp.839-844.

[8] O. Masory and J. Wang, "Workspace Evaluation of Stewart Platforms", *Advanced Robotics, the International Journal of the Robotics Society of Japan*, Vol.9, No.4, 1995, pp.443-461.

[9] P.Huynh and T. Arai, "Kinematic Performance Characteristics for Parallel Manipulators", *Fifth IASTED International Conference on robotics and Manufacturing*, Cancún, Mexico, May 29-31, 1997.

[10] J.P. Merlet, "Détermination de l'espace de travail d'un robot parallèle pour une orientation constante", *Mechanism and Machine Theory*, Vol.29, No.8, 1994, pp.1099-1113.

[11] J. Bessala, et al., "Analytical study of Stewart platforms workspaces", *Proceedings of the International Conference on Robotics and Automation*, Minneapolis, Minnesota, April 1996.

[12] J.P. Merlet, "Parallel Manipulator, Part 2: Singular Configurations and Grassmann Geometry", *INRIA Research Report*, No.791, Feb. 1988.

[13] J.P. Merlet, "Singular Configurations of Parallel Manipulators and Grassmann Geometry", *The International Journal of Robotics Research*, Vol.8, No.5, Oct. 1989, pp.45-56.

[14] P. Huynh and T. Arai, "Maximum Velocity Analysis of Parallel Manipulators", *Proceedings of the International Conference on Robotics and Automation (ICRA'97)*, Albuquerque, New Mexico, USA, April, 1997, pp.3268-3273.

[15] D. Stewart, "A platform with six degrees of freedom", *Proceedings of the Institution of Mechanical Engineers*, Vol.180, Part 1, No.5, 1965-66, pp.371-386.

[16] T. Arai et al., "Development of a New Parallel Manipulator with Fixed Linear Actuator", *Proceedings of the Japan-USA Symposium on Flexible Automation*, Boston, USA, July 7-10, 1996, pp.145-149.

[17] P. Huynh et al., "Optimal Velocity Based Control of a Parallel Manipulator with Fixed Linear Actuators", *Proceedings of the IEEE/RSJ International Conference on Intelligent Robot and Systems*, Grenoble, France, Sept. 7-11,1997, pp.1125-1130.

[18] E.F. Fichter, "A Stewart Platform-Based Manipulator: General Theory and Practical Construction", *The International Journal of Robotics Research*, Vol.5, No.2, Summer 1986, pp.157-182.

[19] K. Cleary and T. Arai, "A prototype parallel manipulator: kinematics, construction, software, workspace results, and singularity analysis", *Proceedings of the International Conference on Robotics and Automation*, Sacramento, CA, April 1991, pp.566-571.

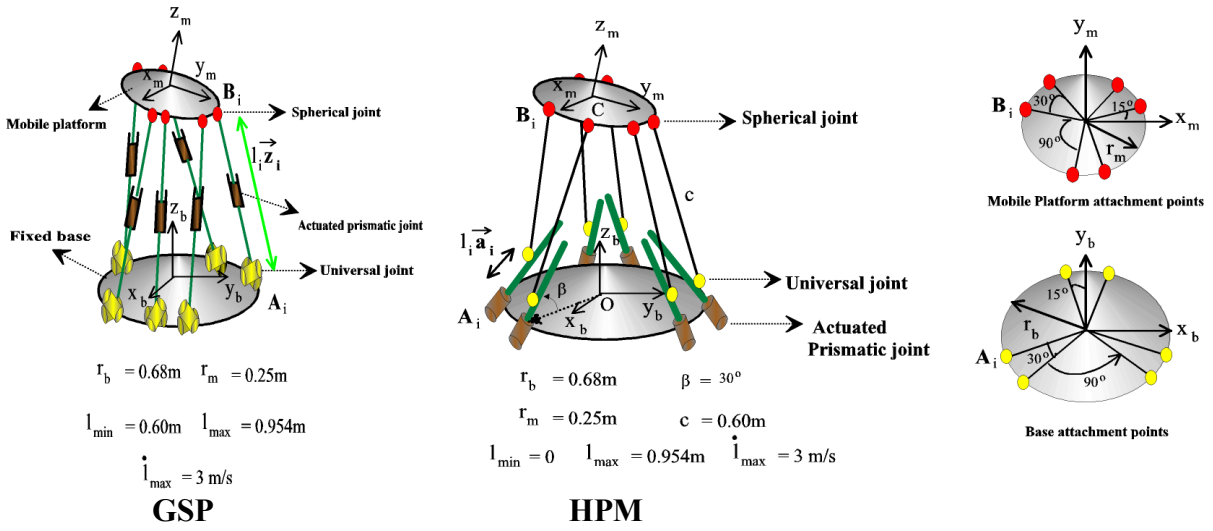

Fig. 5: *Geometric model of the two parallel mechanisms*

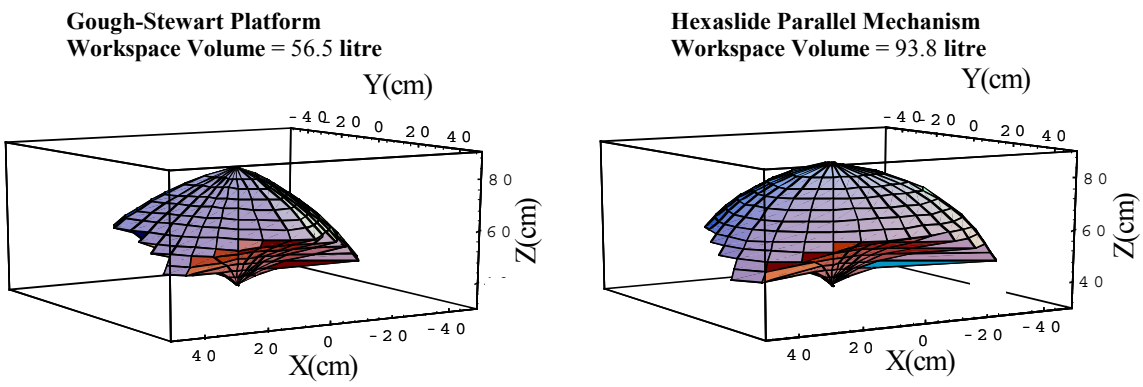

Fig. 6: *Workspace comparison between the two parallel mechanisms*

Gough-Stewart Platform	Hexaslide Parallel Mechanism
$\|\dot{\mathbf{x}}_{max}\| = 5.53\ \mathbf{m/s}$ Surface = 79.23 $\mathbf{(m/s)^2}$	$\|\dot{\mathbf{x}}_{max}\| = 5.09\ \mathbf{m/s}$ Surface = 72.24 $\mathbf{(m/s)^2}$

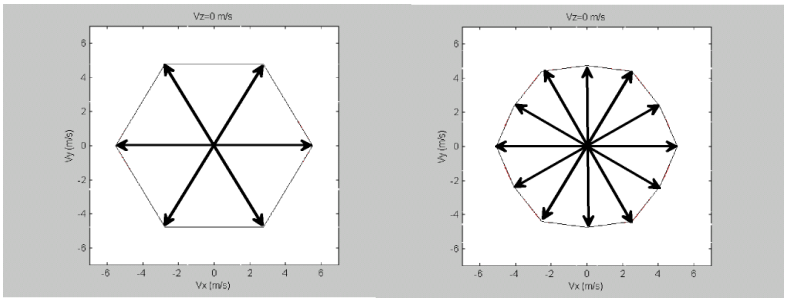

Nominal position: ($x_c = y_c = 0$; $z_c = 0.596$m), ($\psi = \theta = \varphi = 0$) with ($\omega_x = \omega_y = \omega_z = 0$), ($v_z = 0$)

Fig. 7: *Maximum velocity comparison between the two parallel mechanisms in nominal position*

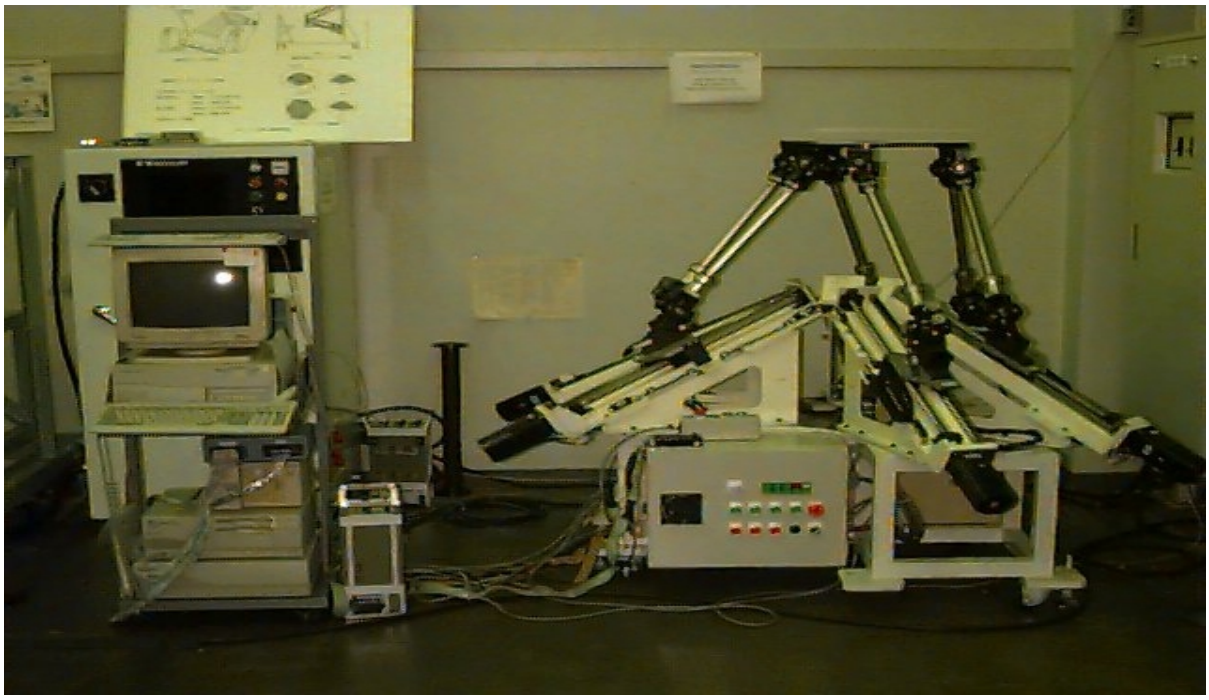

Fig. 8: *Hexaslide Parallel Manipulator*

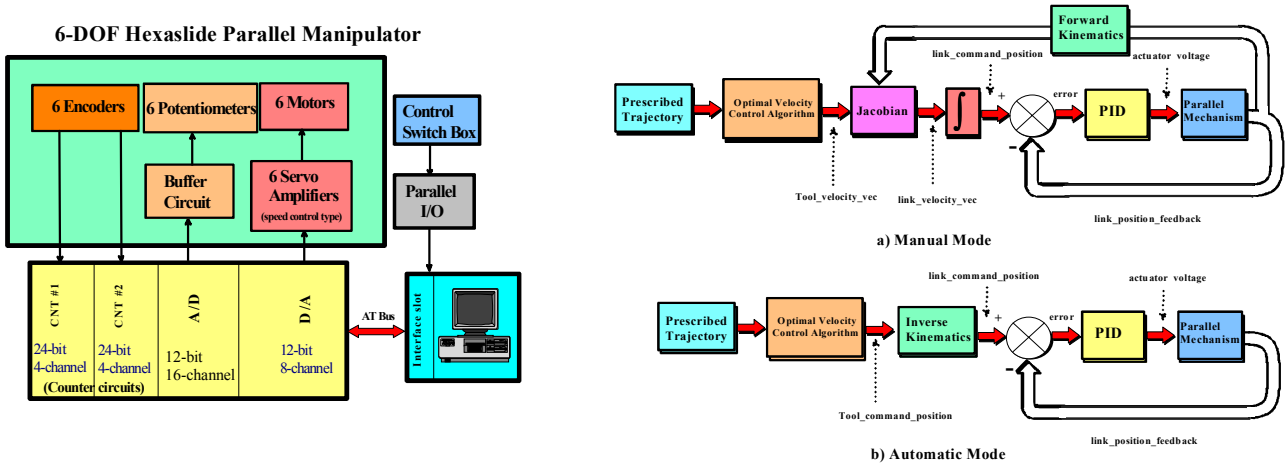

Fig. 9: *Controller Architecture*